

POLARIZED LIGHT PROPAGATION IN HIGHLY SCATTERING TURBID MEDIA
WITH A DISTRIBUTION OF THE PARTICLE SIZE:
A MONTE CARLO STUDY

A Senior Honors Thesis

by

WONSHILL KOH

Submitted to the Office of Honors Programs
& Academic Scholarships
Texas A&M University
in partial fulfillment of the requirements of the

UNIVERSITY UNDERGRADUATE
RESEARCH FELLOWS

April 2002

Group: Engineering

POLARIZED LIGHT PROPAGATION IN HIGHLY SCATTERING TURBID MEDIA
WITH A DISTRIBUTION OF THE PARTICLE SIZE:
A MONTE CARLO STUDY

A Senior Honors Thesis

by

WONSHILL KOH

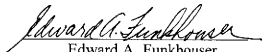
Submitted to the Office of Honors Programs
& Academic Scholarships
Texas A&M University
in partial fulfillment for the designation of

UNIVERSITY UNDERGRADUATE
RESEARCH FELLOW

Approved as to style and content by:



Lihong Wang
(Fellows Advisor)



Edward A. Funkhouser
(Executive Director)

April 2002

Group: Engineering

ABSTRACT

Polarized Light Propagation in Highly Scattering Turbid Media with a Distribution of the Particle Size: A Monte Carlo Study. (April 2002)

Wonshill Koh
Biomedical Engineering Program
Texas A&M University

Fellows Advisor: Dr. Lihong Wang
Biomedical Engineering Program

The light propagation in highly scattering turbid media composed of the particles with different size distribution is studied using a Monte Carlo simulation model implemented in Standard C. Monte Carlo method has been widely utilized to study the propagation of light in turbid media with scattering particles because of its effectiveness and accuracy in approaching photon transport in turbid media. The existing Monte Carlo model developed at the Optical Imaging Lab at Texas A&M University has been extended so that several different size distributions of particles can be considered simultaneously in the propagation of light with two different incident polarization states in two different scattering regions—Mie region and Rayleigh region.

The Monte Carlo model simulation produces optical parameters of polarized light, such as the Stokes vector, the Degree of polarization (DOP), the Degree of linear polarization (DOLP), and the Degree of circular polarization (DOCP), which all provide us with optical information of a given turbid medium. The analysis of these optical characteristics shows that, in Mie region, the light propagation is affected by both the incident polarization states and the size distribution. In Rayleigh region, however, the

size distribution of the particles does not have a significant effect on the optical characteristics of polarized light.

DEDICATION

To my parents, Jungwon Cha and Jimoon Koh,
for their love and support.

ACKNOWLEDGMENTS

I would like to thank Dr. Lihong Wang, for his continuous advice and support. Working at his lab has given me such an exciting opportunity to learn so many new things in the area of Optics. It has been an unforgettable experience that has made me realize once more how exciting and rewarding research can be.

I would like to thank Xueding Wang, a Ph.D. student at the Optical Imaging Lab. He has been kind and generous in answering all my questions and has helped me throughout the whole year since I started with this research with very limited knowledge in Optics.

I would also like to thank Dr. Hsin-i Wu, who taught me the basic concepts in Optics during the summer prior to my research. I would have been so lost without taking an independent study with him.

Finally, I would like to thank my parents for giving me such a rare opportunity to explore the world and for supporting me on everything I do. I also thank my big sister who has always watched over me and been there for me. Thank you, Mom and Dad, for making me try harder to bring out the best in everything I do.

TABLE OF CONTENTS

	Page
ABSTRACT	iii
DEDICATION	v
ACKNOWLEDGMENTS	vi
TABLE OF CONTENTS	vii
LIST OF FIGURES	ix
LIST OF TABLES	xi
CHAPTER	
I INTRODUCTION	1
II PRIOR WORK	4
III MATERIALS AND METHOD	6
A. Theory.....	6
B. Methodology.....	11
IV RESULTS	21
A. Effect of Different Deviation on the Degree of Polarization	21
B. Final Polarization State of Light.....	24
C. Final Stokes Vector Pattern	29
V ANALYSIS	34
A. Effect of Different Deviation on the Degree of Polarization	34
B. Final Polarization State.....	35
C. Final Stokes Vector.....	36
D. Further Study for Horizontally Polarized Light in Mie region: the effects of the center radius and Mie size on the DOP.....	36
VI CONCLUSION	45

	Page
REFERENCES.....	47
VITA	49

LIST OF FIGURES

FIGURE	Page
1	The geometry of the light scattering [12]..... 8
2	The flow chart for the Monte Carlo model simulation..... 15
3	Determining the path of the photon when $s > 1$, (a) The photon exits the sample (b) The photon is bounced back to the sample..... 16
4	Determining the path of the photon when $s < 1$ 17
5	Size distribution of the particles in (a) Mie Region and (b) Rayleigh region..... 18
6	The degree of polarization of (a) horizontally polarized light and (b) circularly polarized light in Mie Region..... 22
7	The degree of polarization of (a) horizontally polarized light and (b) circularly polarized light in Rayleigh region..... 23
8	The final polarization state of (a) horizontally polarized light and (b) circularly polarized light in Mie Region..... 25-26
9	The final polarization state of (a) horizontally polarized light and (b) circularly polarized light in Rayleigh region..... 27-28
10	The final Stokes vector of (a) horizontally polarized light and (b) circularly polarized light in Mie Region..... 30-31
11	The final Stokes vector of (a) horizontally polarized light and (b) circularly polarized light in Rayleigh Region..... 32-33

FIGURE	Page
12	The DOP against the X-axis..... 37
13	Comparison of the DOP by 21 different-sized particles to the DOP by the individual particles for $Dev=0.06*(1.9e-7)$40-41
14	Comparison of the DOP by 21 different-sized particles to the DOP by the individual particles for $Dev=0.3*(1.9e-7)$41-42
15	The original DOP and the net DOP..... 44

LIST OF TABLES

TABLE		Page
I	Input optical parameters.....	13
II	The distribution of the particle size.....	39

CHAPTER I

INTRODUCTION

The optical properties of tissues often provide us with important information about their nature, which can be utilized in diagnostic and therapeutic applications in medicine. As most of biological tissues are turbid media composed of various molecules, studying the propagation of light in turbid media with scattering particles has drawn a lot of interest. The optical properties of these turbid media can be determined by studying the tissue-light interaction whose process can be expressed as the multiplication of the Mueller Matrix with the Stokes vector [1]. The mathematical representation, often in forms of matrices, has been widely used in study of optics by making complex process of light polarization through the optical elements easier to understand, ever since G.G. Stokes introduced Stokes elements to represent polarized light [2].

Although optical imaging has been an important diagnostic tool in medicine for its good contrast, portability, inexpensiveness and non-ionization, the strong optical scattering has also proved to be a challenge in developing better optical imaging. Optical coherence tomography (OCT) and ultrasound modulated optical tomography are some of the new techniques that have been developed to overcome the drawbacks of optical imaging and to enhance its application. Obtaining the optical information of a given medium by analyzing optical characteristics of light is another approach to tissue optics. For example, it is possible to differentiate cancerous cells from non-cancerous

cells by examining the elements of the Mueller matrix of each sample. The Mueller matrix is constructed by recording the intensity of light scattering throughout cancerous cells and non-cancerous cells. This result proposes many other possible uses of the Mueller matrix in biomedicine [3].

Despite an increasing interest in the light polarization in media with highly scattering particles and several investigations to study the optical characteristics of light in turbid media, systemic and numerical analysis of optical characteristics of the polarized light in media composed of different-sized scatterers with different size distribution has not been carried out to date. All previous studies have been performed under the assumption that the size of scatterers in the medium is uniform. The possibility that the turbid medium may contain several types of particles with different sizes at the same time has not been considered. However, it is important to consider the size distribution of particles in media since human tissues seldom contain organelles with only one size.

Hence, in this study, the polarization characteristics of human tissues composed of scatterers with different size distribution is systemically and numerically analyzed using a Monte Carlo simulation model implemented in Standard C. The existing Monte Carlo model developed at the Optical Imaging Lab at Texas A&M University has been extended so that several different size distributions of the particles can be considered simultaneously in the propagation of light with two different incident polarization states [4]. The extended model then traces the polarization state, the intensity, and the position of each photon propagating in the turbid media with different-sized scatterers in two

different scattering regions—Mie region where the size of particle is much larger than wavelength, and Rayleigh region where the size of particle is much smaller than the wavelength. The simulation produces important optical parameters, such as the Mueller matrix, the Stokes vector, the Degree of polarization (DOP), the Degree of linear polarization (DOLP), and the Degree of circular polarization (DOCP), that provide us with optical information of media. These optical parameters are then analyzed to examine how different deviation, which results in the different size distribution of particles, affects the degree of polarization, the final polarization state, and the final Stokes vector of highly scattered light with incident horizontal and circular polarization states.

CHAPTER II

PRIOR WORK

Several numerical and experimental studies have been carried out to examine the light polarization in media with highly scattering particles by analyzing optical characteristics of the polarized light [4, 7, 8, 9]. In numerical studies, Monte Carlo method has been utilized to study the propagation of light in turbid media since it offers a satisfying and effective approach to photon transport in turbid media [5, 6].

Bicout *et al* numerically studied the polarization of light in a multiply scattering medium that contains spherical particles through the SLAB Monte Carlo simulation. The mean diameters of particles simulated were 0.22, 0.48, and 1.05 μm , respectively. They then studied how the size of particles and the initial polarization state of light affect the characteristic length of depolarization. They found that the characteristic length of depolarization of light that is linearly polarized is greater than that of light that is circularly polarized in Raleigh region. In Mie region, the opposite observation was made. [7]

Another Monte Carlo study was done to analyze the multiple scattering of right circularly polarized light in medium with scattering particles. Some of polarization parameters were calculated by varying the size of scattering particles and the thickness of medium. It was found that these optical parameters strongly depend on the size of the particles and the thickness of the sample. [8]

Following the experiment that differentiated cancerous cells from non-cancerous cells through their elements of the Mueller matrix, Bartel and Hielsher numerically

studied the polarization of light that is diffusely backscattered from highly scattering media using a Monte Carlo method. Their model employs the Stokes-Mueller formalism using Mie theory to compute all elements of the diffuse backscattering Mueller matrix of light. Their simulated results matched closely with those from their experiment. [9]

Yao and Wang simulated the steady-state backscattering Mueller matrix of a turbid medium using a time-resolved Monte Carlo technique. Their Monte Carlo model, also based on the Stokes-Mueller formalism, showed the DOP propagation of right-circularly and horizontally polarized incident light. They found that the propagation of DOP is affected by both the incident polarization state of light and the size of scatterers. [4]

Although these studies provide more information about the propagation of polarized light in randomly scattering media, they all pose one limitation in that the size distribution of the particles has not been considered. To overcome this limitation, the Monte Carlo model previously developed by Yao and Wang is further modified so that the program can be simulated in turbid media composed of scattering particles with different size distribution.

CHAPTER III

MATERIALS AND METHOD

A. Theory

Monte Carlo simulations of photon transport in turbid tissues offer a flexibility and accuracy in performing multiple physical quantities simultaneously [5, 6]. Monte Carlo simulations were first introduced into the field of laser-tissue interactions by Wilson and Adam [5]. Since then Monte Carlo simulations of light transport in tissues have been used for various applications and attained many improvements [5]. The optical properties of tissues play a vital role in the propagation of polarized light through the tissue sample, which can be measured by analyzing optical characteristics of the transmitted or backscattered light [10]. The optical properties of tissues are described by parameters, such as the absorption coefficient (μ_a), the scattering coefficient (μ_s), the refractive coefficients (n_a and n_b), the anisotropy factor (g), etc. These are the key input parameters that Monte Carlo model simulates.

The Monte Carlo simulation provides us with the optical characteristics of the medium through its output parameters that comprise the Stokes Vector, Muller Matrix, DOP, DOLP, and DOCP of multiply scattered light. Analysis of these results helps us understand how different size distribution of particles affects the optical characteristics of a given sample.

The Stokes vector, \mathbf{S} , is a four-by-one matrix that describes the polarization state of light.

$$\mathbf{S} = \begin{bmatrix} S_0 \\ S_1 \\ S_2 \\ S_3 \end{bmatrix} \quad (1)$$

The first element, S_0 , represents the intensity of the light. The rest of elements, S_1 , S_2 , and S_3 , represent the polarization state of the light. The element, S_1 , usually describes light that is either horizontally or vertically polarized. The element, S_2 , represents the linear polarization state oriented in the direction of ± 45 degrees. The last element, S_3 , is for light that is right or left circularly polarized. [2, 11]

The other important matrix is a four-by-four matrix called the Mueller matrix, \mathbf{M} . Optical characteristics of an optical element that light encounters can be completely illustrated by the sixteen elements of the Mueller matrix.

$$\mathbf{M} = \begin{bmatrix} m_{11} & m_{12} & m_{13} & m_{14} \\ m_{21} & m_{22} & m_{23} & m_{24} \\ m_{31} & m_{32} & m_{33} & m_{34} \\ m_{41} & m_{42} & m_{43} & m_{44} \end{bmatrix} \quad (2)$$

Given an initial Stokes Vector, \mathbf{S}_0 , of incident light, a final Stokes vector, \mathbf{S}' , of light after encountering an optical element can be calculated by simply multiplying the Mueller matrix by the initial Stokes vector.

$$\mathbf{S}' = \mathbf{M} * \mathbf{S}_0 \quad (3)$$

This equation can be expanded to the Stokes-Mueller formalism to describe the light scattering events in turbid media.

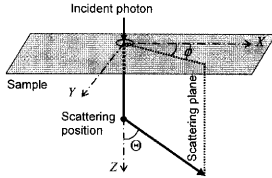


Fig. 1. The geometry of the light scattering [12].

Figure 1 represents the slab geometry of the light scattering that is used for the simulation. The incident photon is placed at the origin $(0, 0, 0)$ of the laboratory coordinate system [12]. The light beam then travels into the sample along the Z-axis. Once the light beam is injected into the sample, the scattering events occur as the light encounters the particles. The polar angle, Θ , ranges from 0 to π while the rotation angle, Φ , ranges from 0 to 2π . These two deflection angles are selected statistically according to Mie theory whose details are described in Ref. 9.

Once Θ and Φ are chosen, the Stokes vector of light after the first scattering can be obtained by,

$$\mathbf{S}' = \mathbf{R}(-\Phi) * \mathbf{M}(\Theta) * \mathbf{R}(\Phi) * \mathbf{S}_0 \quad (4)$$

where \mathbf{R} = Rotation matrix
 \mathbf{M} = Scattering matrix

When the scattering event occurs, the location of the light beam is traced using the local coordinate system as it changes its direction according to two deflection angles. To

locate the final position of the light beam on the laboratory coordinate system, $\mathbf{R}(-\Phi)$ is multiplied at the end to transform the local coordinate system back to the laboratory coordinate system.

Likewise, for the multiple light scattering, the Stokes vector of light can be obtained by multiplying the successive matrices that describe the scattering events with the Stokes vector of the incident polarization state. For example, the final Stokes vector of light that is scattered n times during the propagation can be calculated by,

$$\mathbf{S}' = \mathbf{R}(-\Phi_i) * \mathbf{M}(\Theta_n) * \mathbf{R}(\Phi_n) * \dots * \mathbf{M}(\Theta_1) * \mathbf{R}(\Phi_1) * \mathbf{S}_0$$

where $\Theta_n =$ rotation angle after n^{th} light scattering ,
 $\Phi_n =$ polar angle after n^{th} light scattering ,... (5)
 $\Theta_1 =$ rotation angle after 1^{st} light scattering
 $\Phi_1 =$ polar angle after 1^{st} light scattering .

$\mathbf{R}(-\Phi_i)$ is multiplied to convert the local coordinate system back to the laboratory coordinated system after light is multiply scattered.

\mathbf{M} is the scattering matrix that contains four independent elements, $a(\Theta)$, $b(\Theta)$, $d(\Theta)$, and $e(\Theta)$. Several standard programs are available for calculating their values and an example of their computations can be found in Ref. 9. These programs are based on Mie theory that was developed by Gustav Mie to study scattering of light by homogeneous and isotropic spherical objects [13].

$$\mathbf{M}(\Theta) = \begin{bmatrix} a(\Theta) & b(\Theta) & 0 & 0 \\ b(\Theta) & a(\Theta) & 0 & 0 \\ 0 & 0 & d(\Theta) & -e(\Theta) \\ 0 & 0 & e(\Theta) & d(\Theta) \end{bmatrix} \quad (6)$$

\mathbf{R} is the rotation matrix, which is represented by,

$$\mathbf{R}(\Phi) = \begin{bmatrix} 1 & 0 & 0 & 0 \\ 0 & \cos(2\Phi) & -\sin(2\Phi) & 0 \\ 0 & \sin(2\Phi) & \cos(2\Phi) & 0 \\ 0 & 0 & 0 & 1 \end{bmatrix} \quad (7)$$

The complete mathematical details behind the Stokes-Mueller formalism can be found in Ref. 9, Ref. 11, Ref. 14 and Ref. 15.

The Stokes-Mueller formalism produces the final Stokes vector for each individual photon at the area of interests. Therefore, when there is more than one photon arriving at an area of interest, the net final Stokes vector, $\bar{\mathbf{S}}^i$, can be obtained by summing up the final Stokes vectors of all the individual photons together.

$$\bar{\mathbf{S}}^i = \sum_{i=1}^n \mathbf{S}_r^i \quad (8)$$

where $n = \text{total number of photons}$

Once the net final Stokes vector is obtained, the average DOP, DOLP, and DOCP of scattered light at the area of interests can be calculated.

The DOP indicates the fraction of the light intensity that is polarized regardless of its polarization state.

$$\text{DOP} = \frac{\sqrt{S_1^2 + S_2^2 + S_3^2}}{S_0} \quad (9)$$

where $0 < \text{DOP} < 1$

The DOLP indicates the fraction of the light intensity that is linearly polarized while the DOCP represents the fraction of the light intensity that is circularly polarized.

$$\text{DOLP} = \frac{\sqrt{S_1^2 + S_2^2}}{S_0} \quad (10)$$

$$\text{DOCP} = \frac{|S_3|}{S_0} \quad (11)$$

B. Methodology

The C code for the Monte Carlo model used for this simulation had been initially developed by Yao and Wang and was modified by X. Wang. Wang *et al* first developed a model of steady-state light in multi-layered tissues (MCML) implemented in standard C in 1995, assuming that tissue is homogeneous. MCML is the first such simulation that is portable to multiple computer platforms. MCML allows the number of tissue layers to be varied at run time by allocating arrays and matrices dynamically. A grid element in MCML can also be dynamically allocated and the coordinates of each grid element's simulated data can be optimized [5]. Since then, their code has been used as a backbone of many other Monte Carlo studies of light scattering in turbid media. The model developed by Yao and Wang examines the propagation of light with different incident polarization states in turbid media with one-sized scattering particles [4]. X. Wang then enhanced the model to account for a size distribution. However, X. Wang's model could simulate only one value of size distribution at a time with one polarization state. Two

different initial polarization states of light need to be simulated for each deviation. Therefore, simulating a deviation value with only one polarization state of light at a time made the simulation process slow and inconvenient for examining the effect of a series of different size distributions of the particles to the light propagation.

Therefore, for this study, the model has been extended furthermore to attain an automated simulation for each different value of radius deviation given a range and a step size of deviation. This modification makes the simulation faster and more efficient compared to the previous model. The extended model enables users not only to modify the number of size deviation whenever he/she wishes but also to simulate the program with different initial polarization states and different values of size distribution simultaneously. Moreover, the part of the model, where storing of the data occurs for each polarization state with a different size distribution, has also been modified. As deviation produces two different data sets according to two different polarization states of light, it is necessary to store each data set in a different file. This allows the users to retrieve a proper data set after simulation to analyze the optical characteristics of light. To achieve this, the model is modified using the conditional reasoning based on the number of size distribution.

The optical properties of the sample, which are the important input parameters for the simulation, are determined based on previous experiments that used suspensions of polyester spheres as the medium (Table I).

Table I. Input optical parameters

	Rayleigh Scattering	Mie Scattering
n_a	1.57	
n_b	1.33	
λ (nm)	770	
Concentration of particles	0.13%	
Mie size	21	
μ_a (cm^{-1})	0.1	
Thickness of the sample (cm)	2	
k_a	0.9	2.03
r_c (m)	$9*10^{-8}$	$1.9*10^{-7}$
μ_s (cm^{-1})	2.58	10.06
g	0.17	0.67

The refractive index of particles, n_a , is 1.57, which is the refractive index of polystyrene. The refractive index of solution, n_b , is 1.33. The concentration of particles in medium is 0.13% and the light has the wavelength, λ , of 770nm *in vacuo*. The thickness of the sample is 2 cm with the infinite width. The absorption coefficient, μ_a , is 0.1cm^{-1} . The value of Mie size is 21, which means that there are twenty-one different-sized particles in the medium except in the case where the deviation is equal to zero. Zero deviation indicates that there is no size distribution among particles. The sample contains particles with one size, the center radius, r_c . The other important parameter is the size factor, k_a , which is given by the equation,

$$k_a = \frac{(2\pi * n_b * r_c)}{\lambda} \quad (12)$$

k_a is an important parameter that determines two different types of region where light scattering occurs. If the value of k_a is less than 1.23, light scattering occurs in Rayleigh

region. Rayleigh region is the area of scattering where the size of particle is much smaller than the light wavelength. One example of Rayleigh scattering is scattering of air molecules, which makes the sky blue. When k_a is greater than 1.23, light scattering is considered as Mie scattering. In Mie region, the size of particles is larger than the wavelength of light [15]. To examine how these different types of scattering affect the propagation of light in the same medium, the program is simulated with two values of k_a , 0.9 and 2.03. A different size factor has an impact on the values of the center radius, the scattering coefficient, μ_s , and the anisotropy factor, g . For Rayleigh region ($k_a=0.9$), the center radius of the particles, r_c , is 9×10^{-8} m with μ_s of 2.58 cm^{-1} and g of 0.17. In Mie region, where k_a is equal to 2.03, the program is simulated with the center radius of 1.9×10^{-7} m, μ_s of 10.06 cm^{-1} , and g of 0.67.

Each step of the simulation is briefly described in the flow chart shown in Fig. 2.

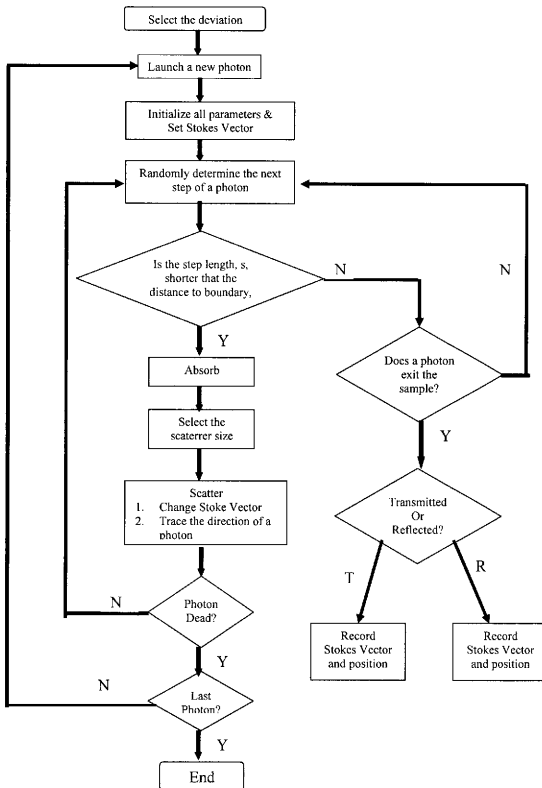


Fig. 1. The flow chart for the Monte Carlo model simulation.

For the first step of the simulation, the program selects a deviation value. Once the deviation is chosen, the first photon is launched by initializing all parameters and setting its Stokes vector for initial polarization state of light.

After launching, the paths of the photon are randomly selected. Selecting the next direction of the photon depends on the step length, s , and distance to boundary, l , of the sample. When s is longer than l , the photon hits the boundary. Upon hitting the boundary of the sample, there are two possibilities that can happen to the photon. If the photon is bounced back to the medium, the photon continues the process of selecting its next path. If the photon is not bounced back to the medium, it then permanently exits the sample through the upper or lower boundary (Fig. 3).

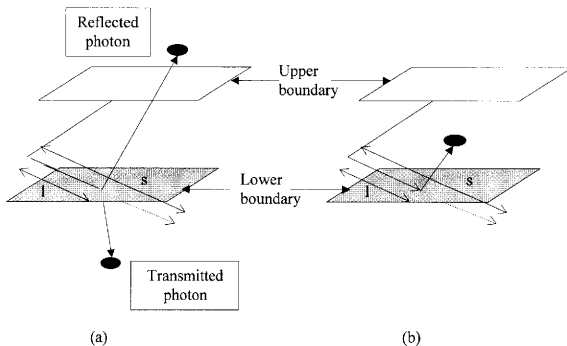


Fig. 3. Determining the path of the photon when $s > l$,
 (a) The photon exits the sample.
 (b) The photon is bounced back to the sample.

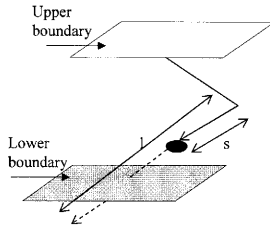


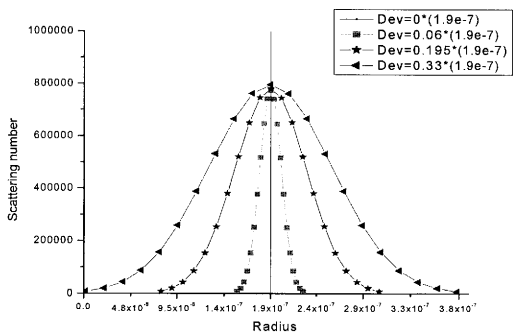
Fig. 4. Determining the path of the photon when $s < l$.

If s is shorter than l (Fig. 4), the photon is absorbed through the medium and then it selects a particle size that it would encounter. Selecting the size of particles is determined by a probability function, p ,

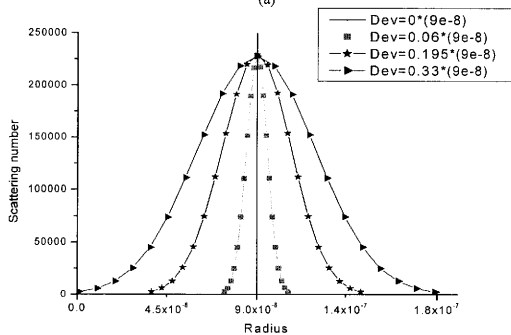
$$p = \frac{1}{\sqrt{2\pi}\sigma} \exp\left[-\frac{(r - r_c)^2}{2\sigma^2}\right] \quad (13)$$

where deviation, $\sigma = \delta * r_c$

The deviation changes as the value of δ varies with a given center radius, r_c . This probability function is set up in a way so that majority of light scattering would occur through the particle with the center radius. The radius range of radius distribution of scatterers gets wider as the deviation increases (Fig. 5).



(a)



(b)

Fig. 5. Size distribution of the particles in (a) Mie Region and (b) Rayleigh region

To choose 21 different sized particles for this simulation, with the center radius being in the middle, the program selects 10 equally distributed radii from the right side of the center radius and the other 10 radii from the left side.

Encountering the selected particle, the photon is scattered. Its direction is traced and the new Stokes vector is recorded using the Stokes-Mueller formalism as described in previous section. After each scattering, the photon is considered dead if its intensity is reduced to less than 0.001% of the original intensity. Otherwise, the photon randomly chooses a new step and repeats its next steps until its intensity gets very weak. When the current photon dies, the next photon is launched and the whole procedure is repeated until the last photon is launched.

For each size factor, the program is simulated to observe the relationship between the degree of polarization and different deviation, and to examine the impact of different size distribution on patterns of the polarization state and the final Stokes vector of multiply scattered light. For the purpose of observing the relationship between the degree of polarization and different deviation, a package of 100,000 photons is launched with twenty-three different values of deviation by varying δ from 0 to 0.33 with a step size of 0.015. For the case of examining the impact of different size distribution on patterns of the polarization state and the final Stokes vector of multiply scattered light, three different values of deviations are considered with δ changing from 0 to 0.33 with a step size of 0.165. The number of photons is increased to 10 million and the thickness of the sample is reduced to 1cm to speed up the process. Based on the statistics of these photon packages, the final Stokes vector is determined and the DOP, DOCP, and DOLP

of highly scattered light with incident horizontal and circular polarization states are calculated.

CHAPTER IV

RESULTS

A. Effect of Different Deviation on the Degree of Polarization

After calculating the DOP, DOLP, and DOCP of multiply scattered light, their values are plotted against different deviation value to observe the relationship between the degree of polarization and different size distribution for light scattered in Mie region (Fig. 6) and Rayleigh region (Fig. 7).

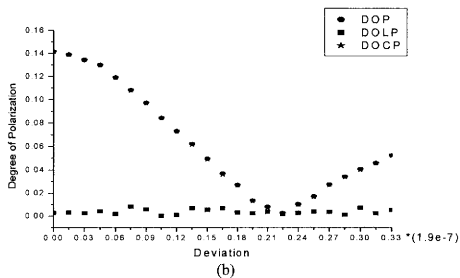
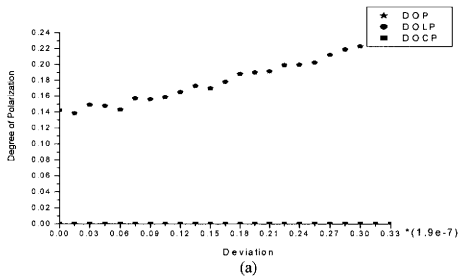
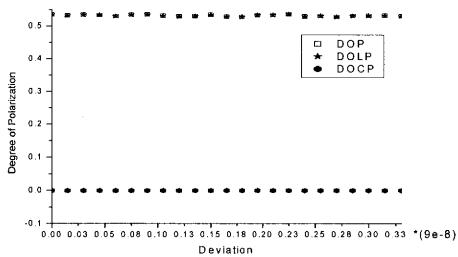
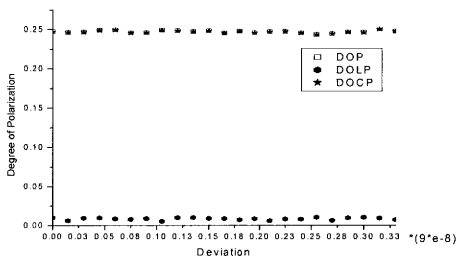


Fig. 6. The degree of polarization of (a) horizontally polarized light and (b) circularly polarized light in Mie Region.



(a)

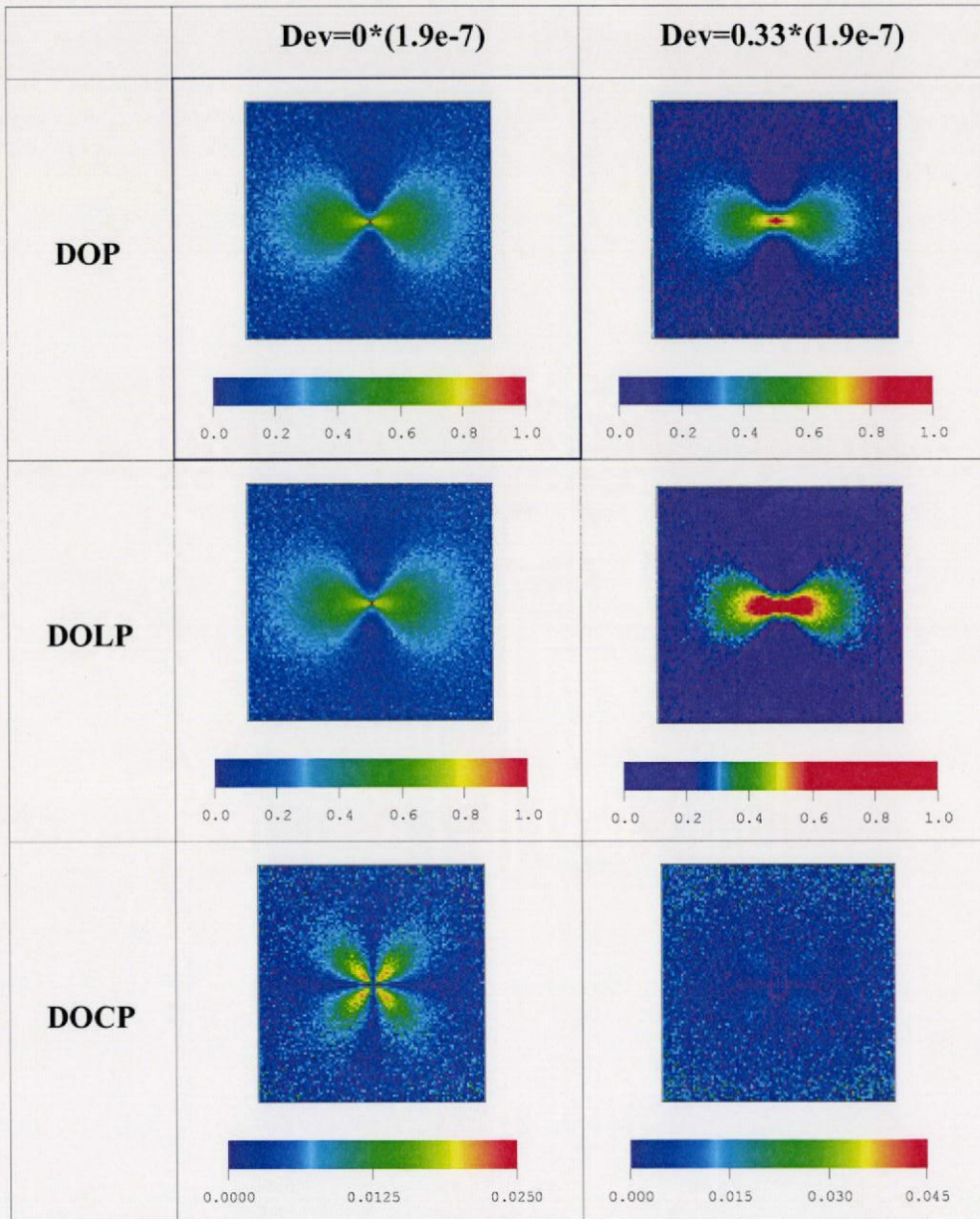


(b)

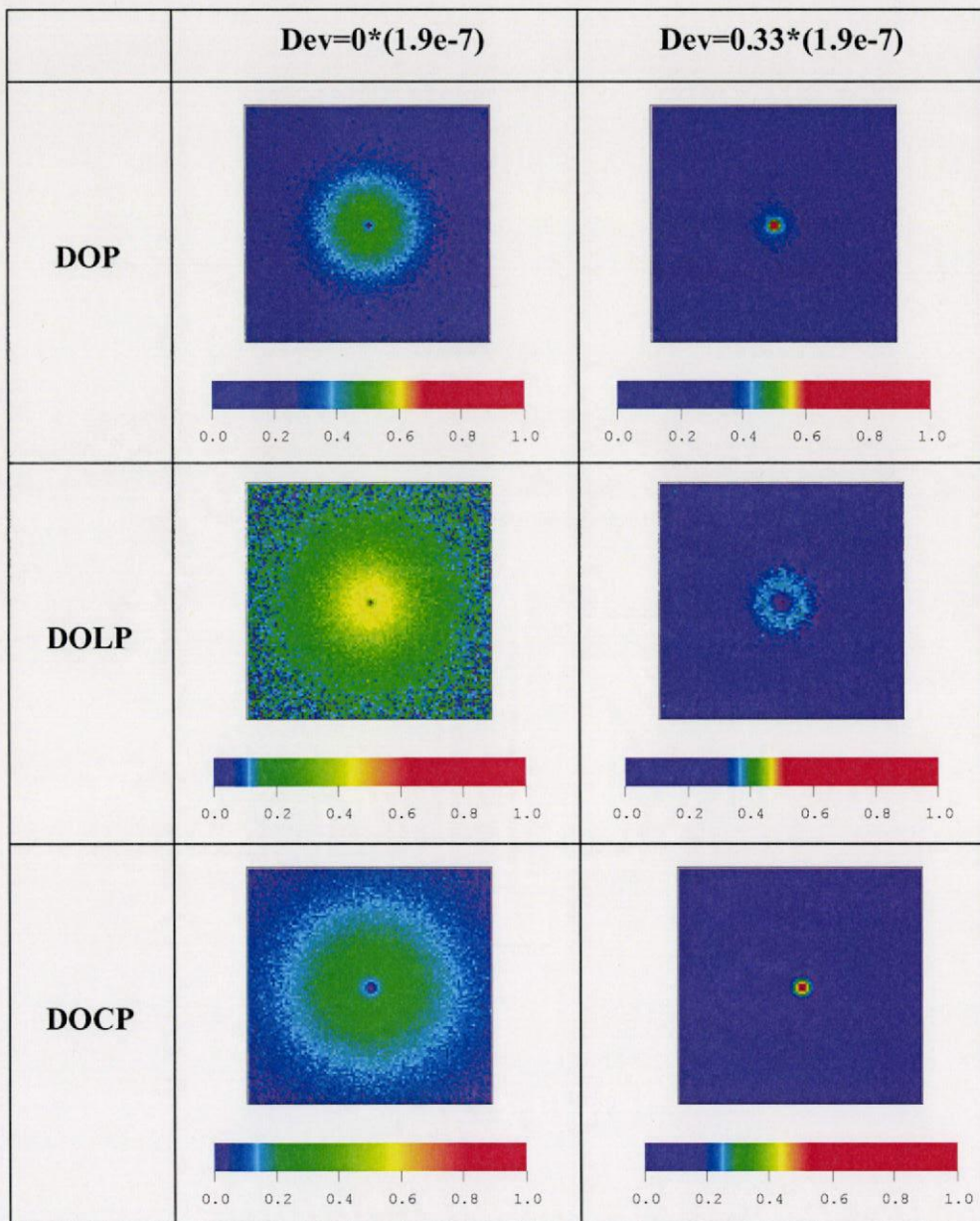
Fig. 7. The degree of polarization of (a) horizontally polarized light and (b) circularly polarized light in Rayleigh region.

B. Final Polarization State of Light

To examine the final polarization state of multiply scattered light, the intensity pattern of the DOP, DOLP, and DOCP are displayed for two different deviation values. When deviation is equal to 0, all particles in the sample have the size of center radius. For the deviation of $0.33*r_c$, the sample contains 21 different sized particles whose sizes are widely distributed. Each intensity pattern is shown as a 2-dimesional image of XY plane over the 2cm by 2cm area at the lower surface of the sample. Figure 8 shows the final polarization state of light scattered in Mie region and Figure 9 describes the final polarization state of light scattered in Rayleigh region.

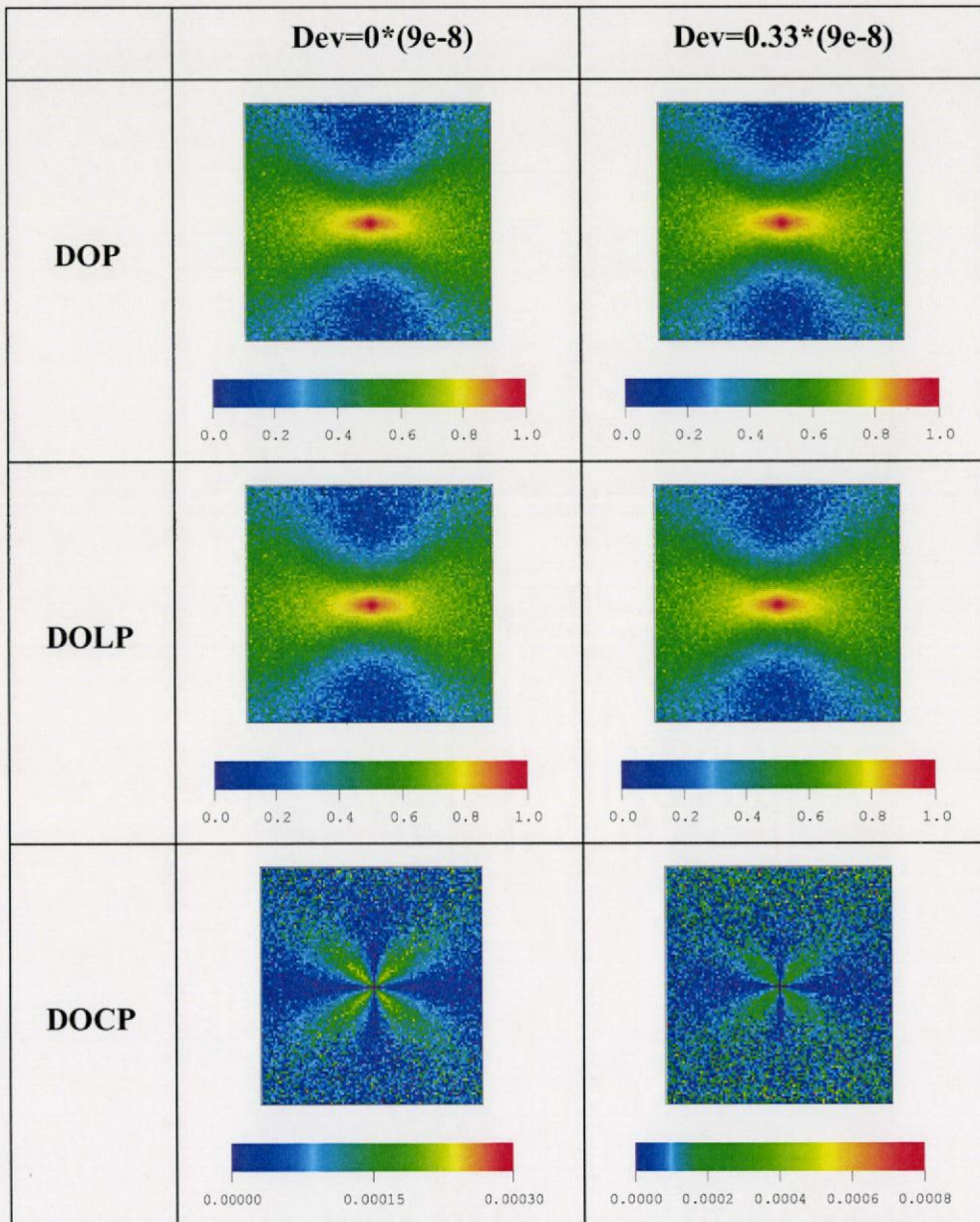


(a)

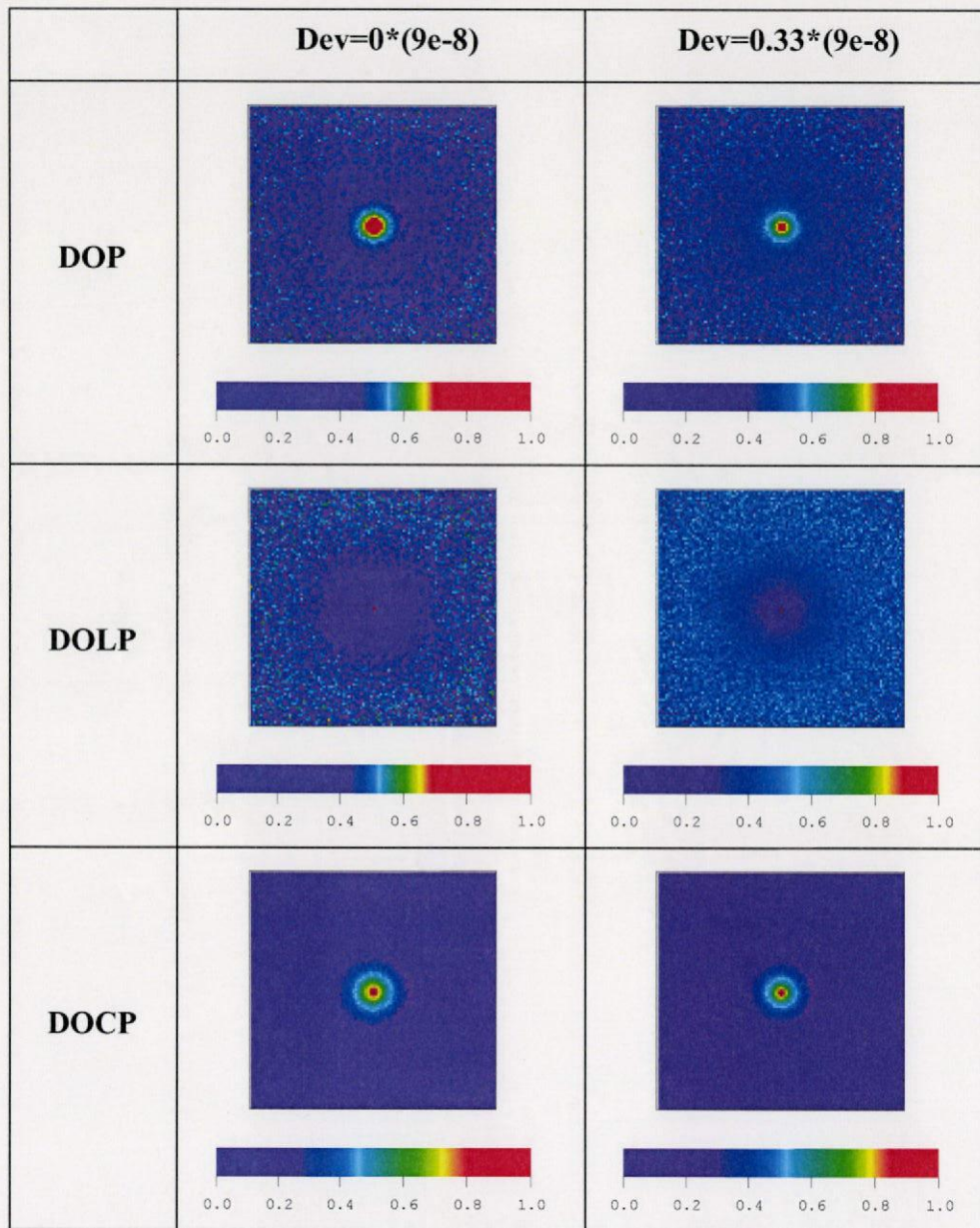


(b)

Fig. 8. The final polarization state of (a) horizontally polarized light and (b) circularly polarized light in Mie Region.



(a)

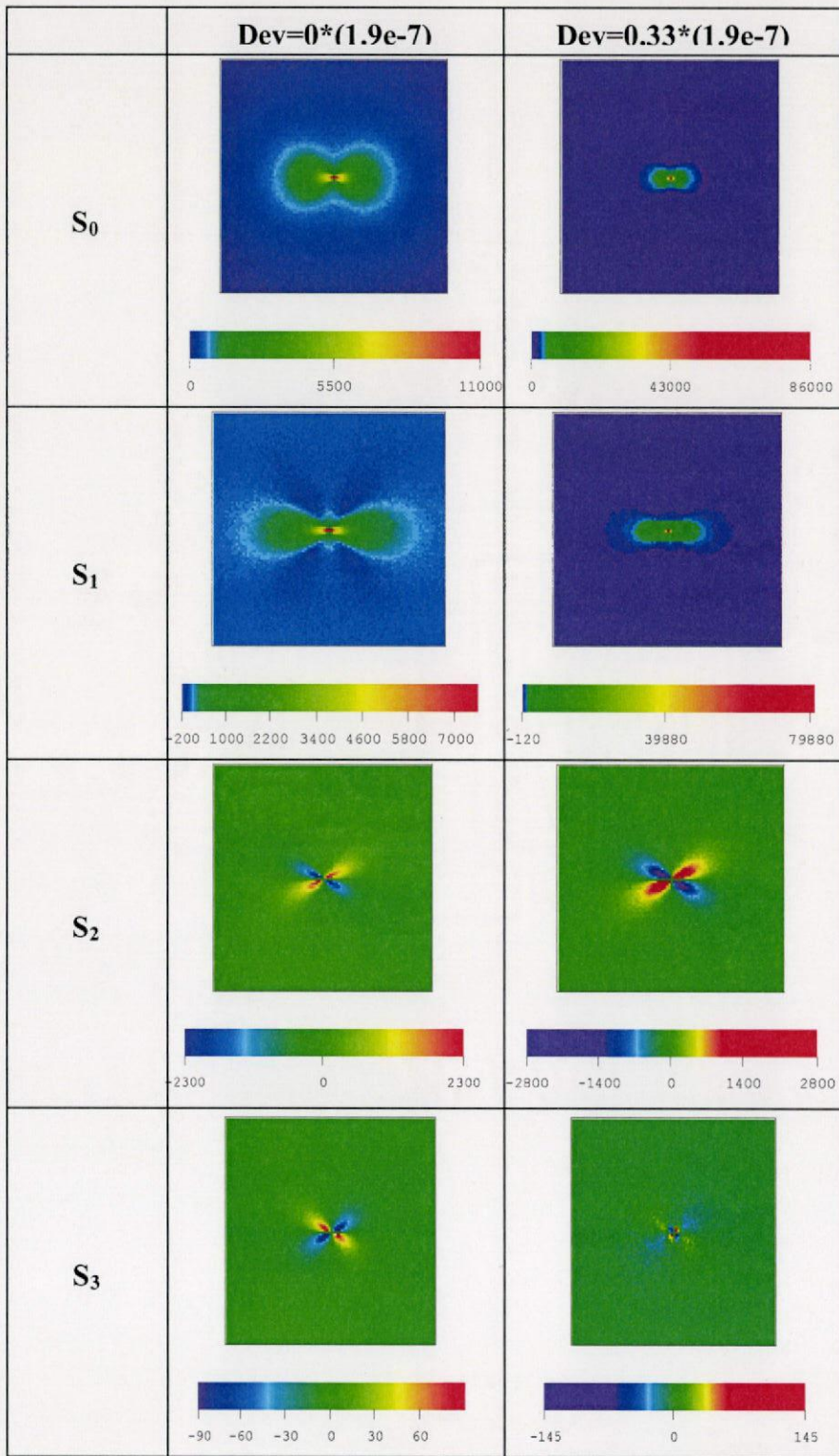


(b)

Fig. 9. The final polarization state of (a) horizontally polarized light and (b) circularly polarized light in Rayleigh region.

C. Final Stokes Vector Pattern

The intensity patterns of each final Stokes vector element are recorded. The final Stokes vector of light scattered in Mie region is displayed in Fig. 10. Figure 11 shows the final Stokes vector of light scattered in Rayleigh region.



(a)

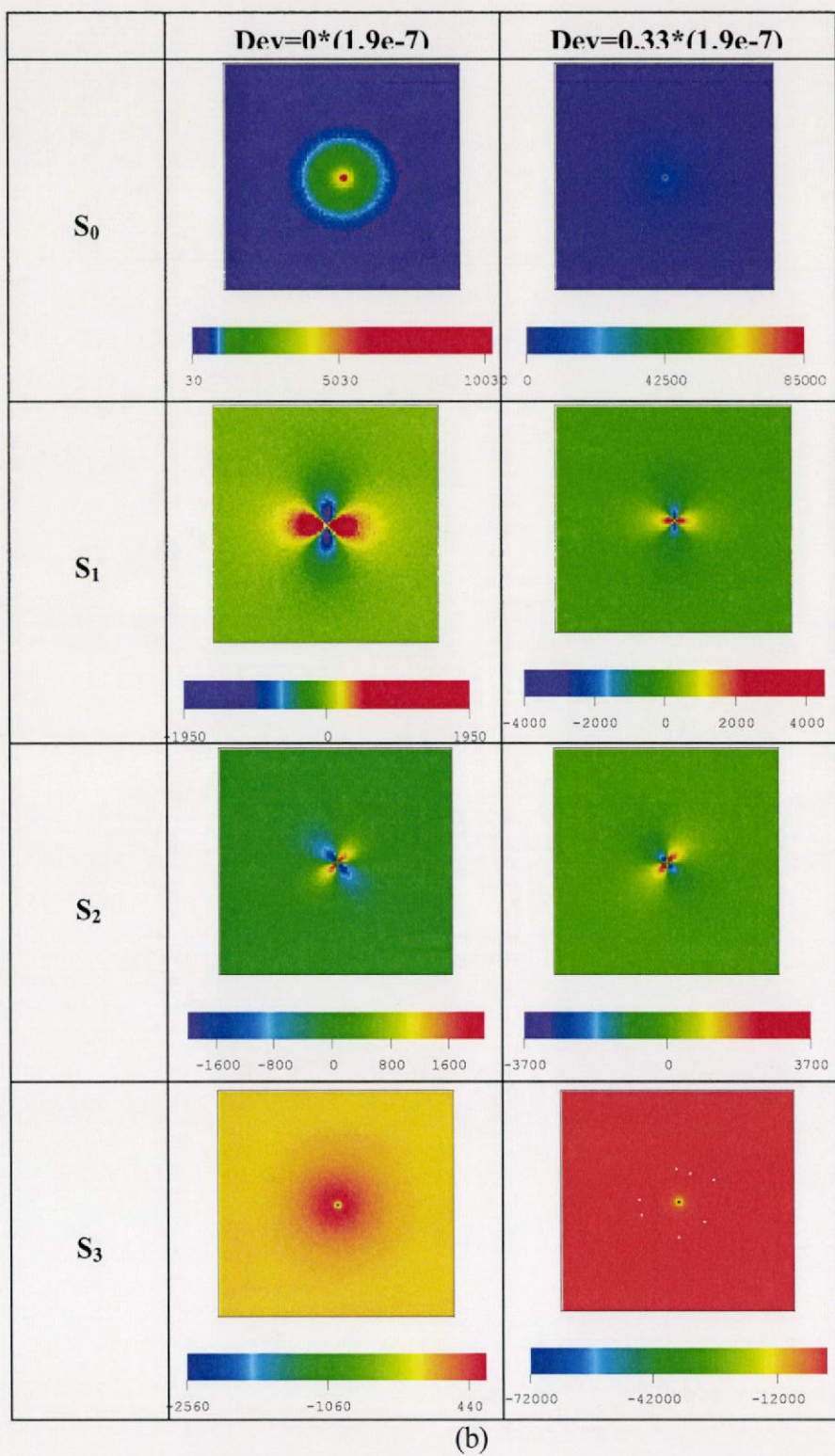
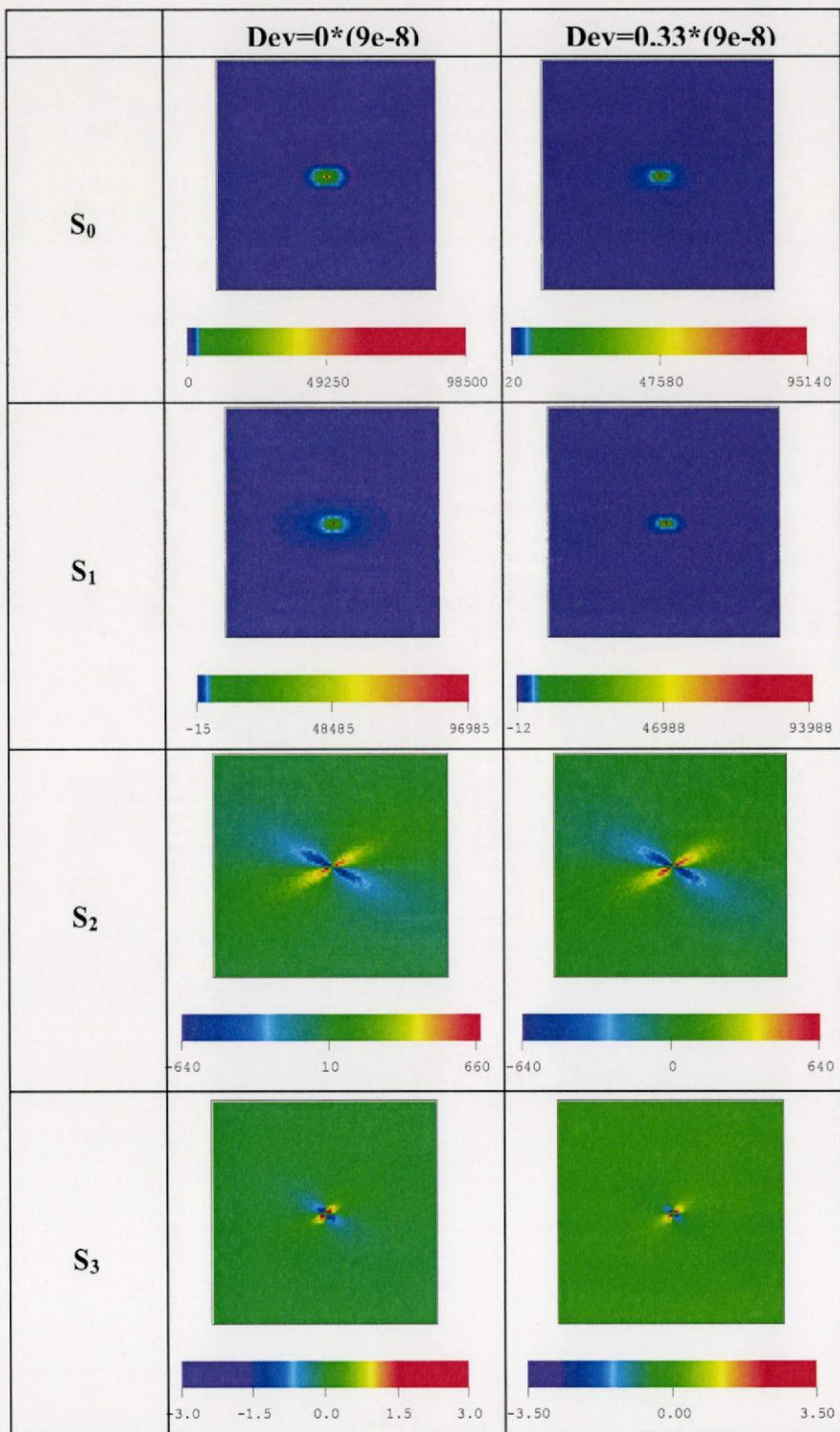


Fig. 10. The final Stokes vector of (a) horizontally polarized light and (b) circularly polarized light in Mie Region.



(a)

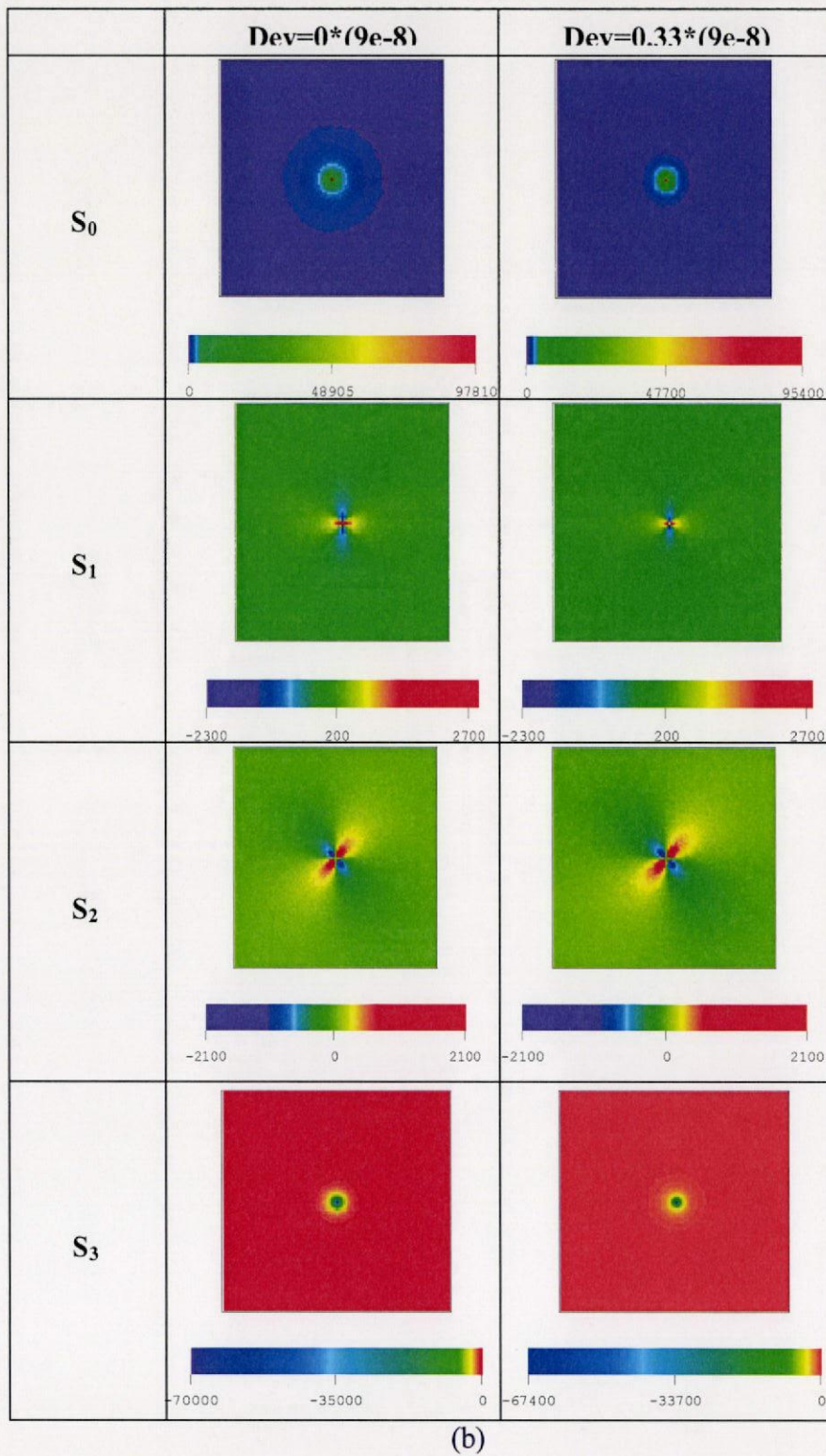


Fig. 11. The Final Stokes vector of (a) horizontally polarized light and (b) circularly polarized light in Rayleigh Region.

CHAPTER V

ANALYSIS

A. Effect of Different Deviation on the Degree of Polarization

Figure 6 (a) shows that there is an increase in the DOP values as δ is incremented from 0 to 0.33, thereby increasing the deviation, for incident horizontally polarized light in Mie region. Since the initial polarization state of light is horizontal, most of the DOP values come from the DOLP with negligible amount coming from the DOCP. For light with incident circular polarization state (Fig. 6(b)), the DOP decreases until δ increases up to 0.21, and then the DOP begins to increase. In this case, most of the DOP values come from the DOCP with the DOLP being almost zero. In contrast to Mie region, there is no significant change in the DOP with different deviation values in Rayleigh region for both horizontally polarized light and circularly polarized light. Therefore, these results indicate that, in Mie region, the degree of polarization is affected not only by initial polarization state of light but also by the size distribution of the particles in media. But, in Rayleigh region, the size distribution of the particles has no significant influence on the degree of polarization of light (Fig. 7). The degree of polarization of light in medium with no size distribution remains almost constant as the size distribution of the particles becomes wider. This shows that the degree of polarization in Rayleigh region is mostly determined by the scattering events of light by the particle that has the center radius regardless of the values of deviation.

B. Final Polarization State

Figure 8 shows the final polarization state of highly scattered light in Mie region. The DOP and DOLP of horizontally polarized light (Fig. 8(a)) are generally distributed along the X-axis for both deviations, $\text{Dev}=0*(1.9\text{e-}7)$ and $\text{Dev}=0.33*(1.9\text{e-}7)$, even though there is a subtle difference in their shape and color distribution depending on the deviation. On the other hand, the intensity pattern of the DOCP is greatly affected by different size distribution of particles. When there is no size distribution among the particles ($\text{Dev}=0*(1.9\text{e-}7)$), the intensity of the DOCP is distributed symmetrically along the diagonals of X- and Y- axes with a shape of clover leaf. When the sizes of the particles are widely distributed ($\text{Dev}=0.33*(1.9\text{e-}7)$), the intensity of the DOCP is randomly distributed within the area with a significant reduction in its intensity. For circularly polarized light in Mie region (Fig. 8(b)), the DOP, DOLP, and DOCP are distributed spherically around the center of the area. Similar to horizontally polarized light, the change of deviation alters the shape and color distribution of the intensity pattern. For scattered light in Rayleigh region (Fig. 9), no significant difference is found in the intensity patterns of the DOP, DOLP and DOCP between two different deviations for both horizontally and circularly polarized light. The intensity patterns of light from the medium with no size distribution look almost the same as those of light from the medium with twenty-one different particles whose sizes are widely distributed. This observation matches with that from part A where it has been found that, in Rayleigh region, it is the particle with the center radius that has the most impact on the propagation of light.

C. Final Stokes Vector

The intensity patterns of final Stokes vector of highly scattered light in Mie region and Rayleigh region are shown in Figs. 10 and 11, respectively. According to the definition of the Stokes vector, the second element, S_1 , indicates the intensity of light that is horizontally/vertically polarized while the fourth element, S_3 , represents the intensity of light that is circularly polarized [2]. Therefore, it was expected that the element S_0 , that describes the total intensity of polarized light, would be mostly determined by the element S_1 for horizontally polarized light, while S_0 would be mostly decided by the element S_3 for circularly polarized light. The intensity patterns in Figs. 10 and 11 prove the assumption to be true in both Mie and Rayleigh regions.

D. Further Study for Horizontally Polarized Light in Mie region: the effects of the center radius and Mie size on the DOP

In parts A and B, it has been found that, for light with incident horizontal polarization state in Mie region, the DOP increases as the size distribution gets wider with the intensity pattern of the DOP being distributed around the X-axis. This indicates that each different deviation somehow affects the DOP distribution along the X-axis. To examine how different deviation affects the DOP along the X-axis, the DOP values from three different deviations are plotted against X-axis while keeping the Y-value constant (Fig. 12).

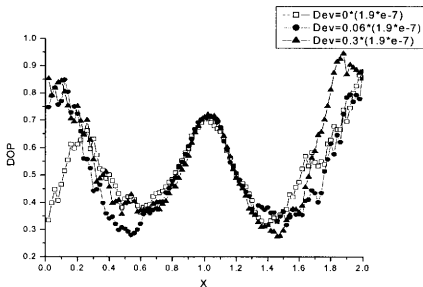


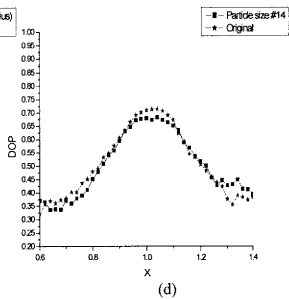
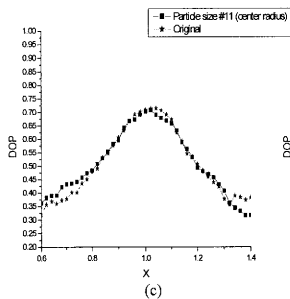
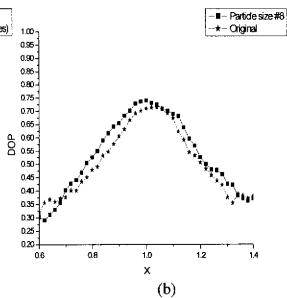
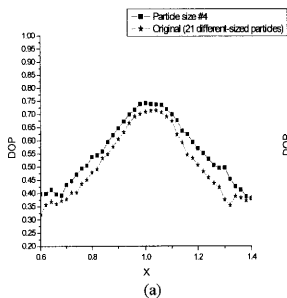
Fig. 12. The DOP against the X-axis.

Figure 12 shows that, in the middle region (from $X=0.6$ to $X=1.4$) of the given 2cm by 2cm area, the DOP distributions by all three deviations are almost identical to each other. In this middle part, the DOP values by three different size distribution remain almost identical to each other. On the contrary, the DOP values around the left and right edges of the given area become higher as the deviation increases. Therefore, given various size distributions, it is the light scattering event occurring at the left and right edges of the area that causes the changes in the DOP for horizontally polarized light in Mie region. Figs. 13 and 14 offer more detailed explanation of the relationship between the DOP by the particle with a center radius alone (no size distribution) and the DOP by the medium with the size distribution in the middle region of the given area. They offer a comparison between the DOP values by the individual-sized particle including the center

radius and the DOP values by all of twenty-one different-sized particles with two different size distributions ($\text{Dev}=0.06*(1.9e-7)$ and $\text{Dev}=0.3*(1.9e-7)$). Five different radii, (size numbers 4, 8, 11, 14, and 18) are selected from two different deviations (Table II). The third radius (size number 11) is the center radius. The simulation is run with the medium composed of only one of these five sized particles at a time and the DOP of light is obtained for each size. Figures 13 and 14 compare the DOP by each individual-sized particle to the original DOP by twenty-one different sized-particles for $\text{Dev}=0.06*(1.9e-7)$ and $\text{Dev}=0.3*(1.9e-7)$, respectively. The X-axis is rescaled so that only the middle region of the area is shown. Both figures show that the DOP of light scattered by the particle with the center radius matches closely to the original DOP of light scattered by twenty-one different-sized particles. The particles with four other size numbers do generate a different DOP value. However, particles with these four other radii have negligible effect on the overall DOP value compared to the particle that has the center radius.

Table II. The distribution of the particle size.

Size number	Dev=0.06*(1.9e-7)		Dev=0.3*(1.9e-7)	
	Radius (m)	Scattering number	Radius (m)	Scattering number
1	1.5580 e-7	8584	1.9000 e-7	8623
2	1.5922 e-7	20162	3.6100 e-8	20402
3	1.6264 e-7	43534	5.3200 e-8	44596
4	1.6606 e-7	85176	7.0300 e-8	87133
5	1.6948 e-7	153316	8.7400 e-8	157312
6	1.7290 e-7	251136	1.0450 e-7	257141
7	1.7632 e-7	377378	1.2160 e-7	386771
8	1.7974 e-7	517232	1.3870 e-7	528218
9	1.8316 e-7	647514	1.5580 e-7	662944
10	1.8658 e-7	742268	1.7290 e-7	757037
11	1.9000 e-7	774228	1.9000 e-7	793538
12	1.9342 e-7	741006	2.0710 e-7	758075
13	1.9684 e-7	645610	2.2420 e-7	662605
14	2.0026 e-7	516635	2.4130 e-7	526797
15	2.0368 e-7	376737	2.5840 e-7	384935
16	2.0710 e-7	250523	2.7550 e-7	257885
17	2.1052 e-7	153559	2.9260 e-7	156791
18	2.1394 e-7	85044	3.0970 e-7	87778
19	2.1736 e-7	43435	3.2680 e-7	44064
20	2.2078 e-7	20582	3.4390 e-7	20720
21	2.2420 e-7	8653	3.6100 e-7	8753



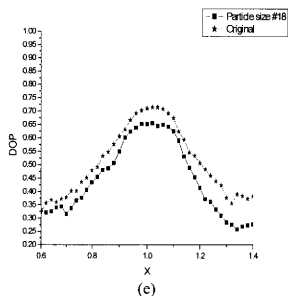
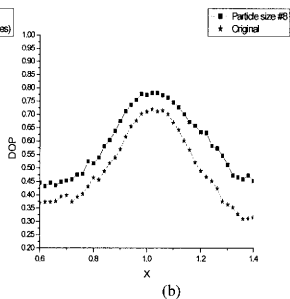
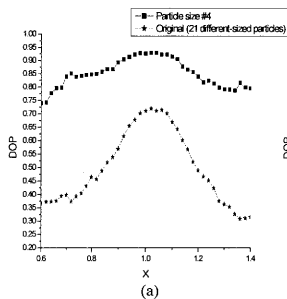


Fig. 13. Comparison of the DOP by 21 different-sized particles to the DOP by the particle with (a) size #4, (b) size #8, (c) size #11, (d) size #14, and (e) size #18 for $\text{Dev}=0.06*(1.9c-7)$.



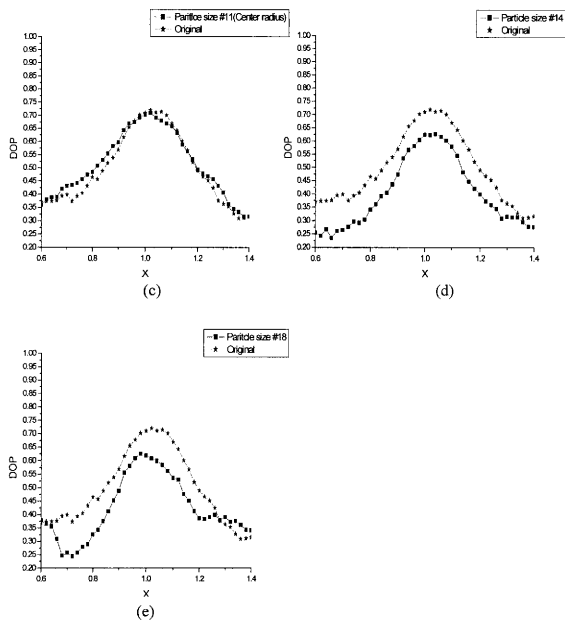


Fig. 14. Comparison of the DOP by 21 different-sized particles to the DOP by the particle with (a) size #4, (b) size #8, (c) size #11, (d) size #14, and (e) size #18 for $Dev=0.3*(1.9e-7)$.

After finding that the particle that has the center radius has most effect on the DOP of light from the medium with various size distributions, it is examined how different values of Mie size affects the DOP of light given two different deviations ($Dev=0.06*(1.9e-7)$ and $Dev=0.3*(1.9e-7)$). With five different radii selected from Table II, the DOP by the individual-sized particle is multiplied with its corresponding weight factor. Their values are then summed up together to obtain the net DOP of light by all of these five different-sized particles.

$$\begin{aligned} \text{Net DOP} = & \text{DOP}_4 * \text{Weight factor}_4 + \text{DOP}_8 * \text{Weight factor}_8 + \\ & \text{DOP}_{11} * \text{Weight factor}_{r_{11}} + \text{DOP}_{14} * \text{Weight factor}_{r_{14}} + \\ & \text{DOP}_{18} * \text{Weight factor}_{r_{18}} \end{aligned} \tag{14}$$

where $DOP_i =$

DOP of light scattered in the medium containing the particle with i^{th} radius

$$\text{Weight factor}_i = \frac{\text{Scattering number for } i^{\text{th}} \text{ radius}}{\text{sum of scattering numbers of 5 radii}}$$

This net DOP is then compared to the original DOP by twenty-one different-sized particles to examine the effect of Mie size to the DOP.

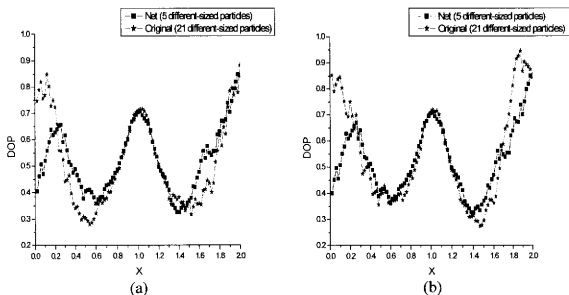


Fig. 15. The original DOP and the net DOP when (a) $Dev=0.06*(1.9e-7)$
 (b) $Dev=0.3*(1.9e-7)$.

Figure 15 shows that, for both deviations, different values of Mie size (5 and 21) yield different DOP values in the left and right boundaries of the given area. When more variety of the particle size is available, light has higher DOP value at the boundary of the given area. Therefore, for horizontally polarized light in Mie region, different values of deviation and Mie size mostly affect the light scattering events that are occurring at the right and left edges of the given area, while the light scattering in the middle region of the area is not influenced by either deviation or Mie size.

CHAPTER VI

CONCLUSION

The light propagation in turbid media composed of different-sized particles has been studied using the Monte Carlo model. The Monte Carlo simulation produces the final optical characteristics of light with incident horizontal polarization state and incident circular polarization state in two different scattering regions—Mie region and Rayleigh region. In Mie region, the size distribution has a significant effect on the degree of polarization, the final polarization state, and the final Stokes vector for both horizontally and circularly polarized light. This study found that the DOP increases as deviation increases for horizontally polarized light. For circularly polarized light, the DOP decreases first before it begins to increase as deviation increases. Different size distribution of the particles also affects the final polarization state that is described through the intensity pattern of the DOP, DOLP, and DOCP. The intensity patterns of each element from the final Stokes vector are also affected by different size distribution. Therefore, the final optical characteristics of polarized light in Mie region are influenced not only by the incident polarization states but also by the size distribution of the particles. Moreover, for light with the incident horizontal polarization state, the differences in the final optical characteristics among different size distribution mainly come from the light scattering events in the right and left boundaries of the given area of the sample. On the contrary, in Rayleigh region, there is no obvious impact of the size distribution on the degree of polarization, the final polarization state, and the final Stokes vector. The optical characteristics of polarized light from the medium with no size

distribution remain almost identical to those from the medium with different size distribution of the particles.

The Monte Carlo model is an effective tool to study the light propagation in turbid media composed of highly scattering particles with the size distribution as it provides us with thorough numerical analysis of optical properties of the medium. The analysis of optical characteristics of polarized light allows us to obtain more detailed insights about optical nature of turbid media with different-sized particles such as our biological tissue. The simulated turbid media in this study is the simplest imitation to our biological tissues assuming all particles to be spheres and their properties to be isotropic. To obtain more complete understanding in optical characteristics of our biological tissues, it is necessary to further extend the Monte Carlo model so that turbid media composed scattering particles whose properties are anisotropic and whose shapes vary including the cylindrical form (shape of muscle fibers) [7].

The results from this Monte Carlo study and their analysis can guide practical experiments in future. The simulation model developed in this study can serve as a basic template for experiment design. Furthermore, this Monte Carlo model can be simulated to validate experimental results whose information might be applied to imaging applications for diagnostic purposes in medicine.

REFERENCES

1. W.S. Bartel and W.M. Bailey, "Stokes vector, Mueller matrix, and polarized scattered light, *Am. J. Phys.* **53**, 468-478 (1985).
2. E. Hecht, *Optics* (Addison-Wesley, New York, 1998).
3. A.H. Hielscher, A.A. Eick, J.R. Mourant, D. Shen, J.P. Freyer, and I.J. Bigio, "Diffuse scattering Mueller matrices of highly scattering media", *Optics Express*, **1**, 441-453 (1997).
4. G. Yao and L. Wang, "Propagation of polarized light in turbid media: simulated animation sequences," *Optics Express*, **7**, 198-203 (2000).
5. L. Wang, S.L. Jacques, and L. Zheng, "MCML – Monte Carlo modeling of light transport in multi layered tissues," *Computer methods and programs in biomedicines*, **47**, 131-146 (1995).
6. L. Wang, S.L. Jacques, and L. Zheng, "CONV-convolution for responses to a finite diameter photon beam incident on multi-layered tissues," *Computer methods and programs in Biomedicine*, **54**, 141-150 (1997).
7. D. Bicout, C. Brosseau, A.S. Martinez, and J.M. Schmitt, "Depolarization of multiply scattered waves by spherical diffusers: Influence of the size parameter," *Physical Review E*, **49**, 1767-1770 (1994).
8. A.H. Hielscher, J.R. Mourant, and I.J. Bigio, "Influence of particle size and concentration on the diffuse backscattering of polarized light from tissue phantoms and biological cell suspension," *Applied optics*, **36**, 125-135 (1997).

9. S. Bartel and A.H. Hielscher, "Monte Carlo simulations of the diffuse backscattering Mueller matrix for highly scattering media," *Applied Optics*. **39**, 1580-1588 (2000).
10. L. Wang and S. L. Jacques, "Error estimation of measuring total interaction coefficients of turbid media using collimated light transmission," *Phys Med Biol*. **39**, 2349-2354 (1994).
11. A. Ambirajan and D.C. Look, "A backward Monte Carlo study of the multiple scattering of a polarized laser beam," *J. Quant. Spectrosc. Transfer*. **58**, 171-192 (1997).
12. X. Wang and L.V. Wang, "Polarized light propagation through the scattering media: time-resolved Monte Carlo and experiments," submitted (2002).
13. H.C. van de Hulst, *Light Scattering by Small Particles* (Dover, New York, 1981).
14. M.J. Rakovic, G.W. Kattawar, M. Mehrubeoglu, B.D. Cameron, L. Wang, S. Rastegar, and G.L. Cote, "Light backscattering polarization patterns from turbid media: theory and experiment," *Applied optics*. **20**, 3399-3408 (1999).
15. C.F. Bohren and D.R. Huffman, *Absorption and Scattering of Light by Small Particles* (John Wiley & Sons, Inc., New York, 1983).

VITA

Wonshill Koh is pursuing a B.S. degree in Biomedical Engineering at Texas A&M University. She will be starting the M.D./Ph.D. Program at Texas A&M Medical School from August, 2002. Permanent Address: 476-10, Shinan-dong, Bukgu #101, Kwangju, South Korea, 500-060.